

THE CRYSTAL STRUCTURE OF EMILITE, $\text{Cu}_{10.7}\text{Pb}_{10.7}\text{Bi}_{21.3}\text{S}_{48}$, THE SECOND 45 Å DERIVATIVE OF THE BISMUTHINITE–AIKINITE SOLID-SOLUTION SERIES

TONČI BALIĆ-ŽUNIĆ[§], DAN TOPA[¶] AND EMIL MAKOVICKY

Geological Institute, University of Copenhagen, Øster Voldgade 10, DK-1350 Copenhagen K, Denmark

ABSTRACT

The crystal structure of the new mineral species emilite, discovered in the Felbertal scheelite deposit, Austria [$\text{Cu}_{10.7}\text{Pb}_{10.7}\text{Bi}_{21.3}\text{S}_{48}$, $Pmc2_1$, a 4.0285(8), b 44.986(9), c 11.599(2) Å], reveals it to be a new 45 Å member of the bismuthinite – krupkaite – aikinite solid-solution series. A refinement of the crystal structure was made with single-crystal measurements, which included 2943 observed unique reflections ($I > 2\sigma_I$) and resulted in $R_1 = 6.6\%$ ($R_W = 22.4\%$). The crystal structure is composed of a fairly complex sequence of krupkaite-like and aikinite-like structure intervals. Emilite is structurally an analogue of the only other 45 Å member of the series, salzburgite ($\text{Cu}_{6.4}\text{Pb}_{6.4}\text{Bi}_{25.6}\text{S}_{48}$). Where one structure has [001] rows of Cu-filled tetrahedra, the other has empty or half-empty tetrahedra, and *vice versa*. The oversubstitution of Cu in the krupkaite-like intervals in the structure causes a departure from an idealized $\text{Cu}_{10}\text{Pb}_{10}\text{Bi}_{22}\text{S}_{48}$ composition and might be required by a metric fit between the krupkaite and aikinite modules in the structure and thus be a prerequisite for its stabilization.

Keywords: emilite, $\text{Cu}_{10.7}\text{Pb}_{10.7}\text{Bi}_{21.3}\text{S}_{48}$, aikinite–bismuthinite derivative, crystal structure, Felbertal, scheelite deposit, Austria.

SOMMAIRE

La structure cristalline de l'émilite, nouvelle espèce minérale provenant du gisement de scheelite de Felbertal, en Autriche [$\text{Cu}_{10.7}\text{Pb}_{10.7}\text{Bi}_{21.3}\text{S}_{48}$, $Pmc2_1$, a 4.0285(8), b 44.986(9), c 11.599(2) Å] montre qu'il s'agit d'un nouveau membre à 45 Å de la solution solide bismuthinite – krupkaïte – aikinite. Un affinement de la structure, fondé sur les mesures faites sur un cristal unique comprenant 2943 réflexions uniques observées ($I > 2\sigma_I$), a donné un résidu R_1 de 6.6% ($R_W = 22.4\%$). La structure contient une séquence relativement complexe d'intervalles ressemblant à la structure de la krupkaïte et à celle de l'aikinite. L'émilite est un analogue du seul autre membre à 45 Å de la série, la salzburgite ($\text{Cu}_{6.4}\text{Pb}_{6.4}\text{Bi}_{25.6}\text{S}_{48}$). Où une structure possède des rangées [001] de tétraèdres contenant les atomes de Cu, l'autre contient des sites tétraédriques vides ou à moitié remplis, et *vice versa*. La sursubstitution du Cu dans les intervalles ressemblant à la krupkaïte mène à un écart à la composition idéalisée, $\text{Cu}_{10}\text{Pb}_{10}\text{Bi}_{22}\text{S}_{48}$, écart qui pourrait bien être requis pour obtenir une concordance métrique des modules de krupkaïte et d'aikinite dans la structure, et donc pour stabiliser la structure.

(Traduit par la Rédaction)

Mots-clés: émilite, $\text{Cu}_{10.7}\text{Pb}_{10.7}\text{Bi}_{21.3}\text{S}_{48}$, dérivé de aikinite–bismuthinite, structure cristalline, Felbertal, gisement de scheelite, Autriche.

INTRODUCTION

The metamorphosed scheelite deposit of Felbertal, Austria, has recently yielded three completely new derivatives of the bismuthinite–aikinite solid-solution series. The crystal structure of the first of these phases, $\text{Cu}_{1.6}\text{Pb}_{1.6}\text{Bi}_{6.4}\text{S}_{12}$ (subsequently named and approved as salzburgite), a fourfold superstructure of Bi_2S_3 , was published by Topa *et al.* (2000). There followed a fivefold

superstructure, $\text{Cu}_{1.7}\text{Pb}_{1.7}\text{Bi}_{6.3}\text{S}_{12}$ (Makovicky *et al.* 2001); it was approved by CNMMN in May 2001 as the new mineral species *paarite*. Both these phases lie compositionally between gladite $\text{CuPbBi}_5\text{S}_9$, a threefold superstructure, and krupkaite $\text{CuPbBi}_3\text{S}_6$, a “stuffed” derivative of Bi_2S_3 .

In this contribution, we deal with the structure of emilite, still another fourfold superstructure of the bismuthinite motif. However, its composition lies be-

[§] E-mail address: tonci@geo.geol.ku.dk

[¶] On leave from the Mineralogical Institute, University of Salzburg, Austria.

tween krupkaite CuPbBiS_3 and hammarite $\text{Cu}_2\text{Pb}_2\text{Bi}_4\text{S}_9$, and it falls between the latter threefold superstructure and the fivefold superstructure of lindströmite, $\text{Cu}_3\text{Pb}_3\text{Bi}_7\text{S}_{15}$.

The possible existence of a four-fold superstructure in this region of the bismuthinite–aikinite solid solution was noted by Pring (1995, Fig. 5) in the annealing and HRTEM study of synthetic hammarite. His figure illustrates occasional single four-fold lamellae disrupting the regular sequence of three-fold hammarite supercells.

The existence of emilite, approved by CNMNM in May 2001, was first noted by Topa *et al.* (2000); its mineralogical description is under preparation, together with descriptions of the two above-mentioned new phases of the bismuthinite–aikinite series. All of them can be distinguished only by means of accurate electron-microprobe analyses and single-crystal diffraction.

EXPERIMENTAL

The chemical composition of two crystals was obtained by electron-microprobe analysis before their extraction from a polished section. We used a JEOL–8600 electron microprobe equipped with Link EXL software with on-line ZAF correction. Analytical conditions employed were 25 kV and 30 nA; synthetic and natural sulfide standards were used. The average result of five point-analyses (wt.%) is Cu 7.68(3), Pb 25.4(1), Bi 49.9(1), S 17.59(4), total 100.6(1)% for the crystal used for the crystal-structure description. Its resulting empirical formula, calculated according to the formalism of Makovicky & Makovicky (1978), is $\text{Cu}_{2.68}\text{Pb}_{2.72}\text{Bi}_{5.30}\text{S}_{12.18}$, *i.e.*, $n_{\text{aik}} = 67.5 \pm 0.5$ (Δn_{aik} , the difference in n_{aik} values if based solely on Cu and on Pb, respectively, is equal to 1.0) or, alternatively, the proportion of the krupkaite end-member is equal to 65.0 mol.%, and that of the aikinite end-member is 35.0 mol.%. For the second crystal, the average result of seven point-analyses (wt.%) is Cu 7.49(5), Pb 24.9(1), Bi 50.1 (3), S 17.48(9), total 100.0(5)%. Its empirical formula is $\text{Cu}_{2.63}\text{Pb}_{2.68}\text{Bi}_{5.34}\text{S}_{12.15}$, *i.e.*, $n_{\text{aik}} = 66.4 \pm 0.6$ ($\Delta n_{\text{aik}} = 1.3$).

Intensity data from the principal crystal, an irregularly shaped fragment $0.04 \times 0.10 \times 0.11$ mm in diameter, was measured on a Bruker AXS four-circle diffractometer equipped with CCD 1000K area detector ($6.25 \text{ cm} \times 6.25 \text{ cm}$ active detection area, 512×512 pixels) and a flat graphite monochromator using MoK α radiation from a fine-focus sealed X-ray tube. The sample–detector distance was fixed at 6 cm. In all, 1800 static exposures 0.3% apart were made, each measurement taking 90 s, with 91.9% coverage and average redundancy of 3.5 inside the limits of the angular span covered. The SMART system of programs was used for unit-cell determination and data collection (Table 1), SAINT+ for the calculation of integrated intensities, and SHELXTL for the structure solution and refinement (all Bruker AXS products). For the empirical absorption correction, based on reflection measurements at differ-

ent azimuthal angles and measurements of equivalent reflections, program XPREP from the SHELXTL package was used, and yielded a merging R_{INT} factor (for equivalents) of 0.0783 compared to 0.1649 before absorption correction. The systematic absences ($h0l$, $l = 2n+1$, and $00l$, $l = 2n+1$) are consistent with space groups $Pmc2_1$ and $Pmcm$. The former was chosen as consistent with structures of the bismuthinite–aikinite family. The structure was solved by direct methods, which suggested a solution revealing the positions of Bi and Pb atoms together with principal Cu sites and the S atoms. In subsequent refinements, the positions of the Cu sites with lower occupancies were deduced from the difference-Fourier syntheses.

The final refinement in $Pmc2_1$ was done with anisotropic displacement-factors used for all the metal atoms except for the partly occupied Cu sites. For the latter, the displacement factors were fixed to isotropic values of $U = 0.04$, whereas for S atoms, the unconstrained isotropic factors were used. The highest residual peak was $4 \text{ e}/\text{\AA}^3$, and the deepest hole $-5 \text{ e}/\text{\AA}^3$. All absolute values of the correlation-matrix elements were lower than 0.6. The refinement was stopped when the maximum shift/e.s.d. for the parameters varied dropped below 1. The results of the refinement are presented in Table 2 and Figure 1, and the interatomic distances, in Table 3 (deposited). Structure factors may be obtained from the Depository of Unpublished Data, CISTI, National Research Council, Ottawa, Ontario K1A 0S2, Canada.

The subsidiary crystal had a considerably smaller volume, $0.08 \times 0.05 \times 0.03$ mm. The number of observed reflections, 2428, is lower than for the principal crystal, R_{int} is 0.105, *i.e.*, higher than for the latter, although about the same volume was sampled in reciprocal space. The resulting agreement-factors ($R = 0.076$, $R_{\text{all}} = 0.1302$, $wR = 0.211$) and the residual $\Delta\rho$ are higher than for the principal crystal (Table 1). As a consequence, the resulting resolution is lower than in the case

TABLE 1. EMILITE: CRYSTAL DATA AND STRUCTURE-REFINEMENT INFORMATION

Bruker AXS four-circle diffractometer	CCD 1000 K area detector
$6.25 \times 6.25 \text{ cm}$ active detection area	512×512 pixels
MoK α radiation, flat graphite monochromator	
Maximum 2θ : 53° ($d = 0.8 \text{ \AA}$)	
Miller index limits h : -5 $+$ 4 ; k : -55 $+$ 54 ; l : -13 $+$ 13	
Measured reflections: 12803	Unique: 3785 (2943 with $I > 2\sigma$)
Temperature: 298 K	Space group: $Pmc2_1$
Unit-cell parameters: a 4.0285(8), b 44.986(9), c 11.599(2) \AA , V 2102.1(7) \AA^3	
(refined from 4150 reflections with $I > 10\sigma$)	
Chemical formula (from structure): $\text{Cu}_{2.36}\text{Pb}_{2.36}\text{Bi}_{10.64}\text{S}_{24}$	
$Z = 4$;	$\rho_c = 7.025 \text{ g/cm}^3$; $\mu = 69.58 \text{ mm}^{-1}$
Empirical absorption correction	
Crystal shape: irregular, 0.04 – 0.11 mm in diameter	
Minimum/maximum transmission factor: 0.0031–0.02208	
Full-matrix refinement	
Twin refinement: Flack parameter 0.50(3)	
Weighting scheme: $1/(\sigma_{F_o}^2 + [0.1(\text{Max}(F_o, 2) + 2F_c^2)/3]^2)$	
R factors: $\{\sum[w(F_o^2 - F_c^2)^2]/\sum[w(F_c^2)^2]\}^{1/2} = 0.2243$; $\sum F_o - F_c /\sum F_o = 0.0661$	
(for $F_o > 4\sigma_{F_o}$), 0.0807 (for all), GooF = 1.459	
Scale factor: 0.0217	

TABLE 2. THE ATOMIC PARAMETERS IN THE STRUCTURE OF EMILITE

Atom	x	y	z	sof	U ₁₁ or U _{iso}	U ₂₂	U ₃₃	U ₂₃	U _{eq}
Bi1	0	0.14354(5)	0.4003(2)	1	0.030(1)	0.027(1)	0.034(1)	-0.005(1)	0.0301(6)
Bi2	0.5	-0.01589(5)	0.3608(2)	1	0.031(1)	0.030(1)	0.027(1)	-0.001(1)	0.0295(6)
Bi3	0.5	0.07152(6)	0.5363(2)	1	0.035(1)	0.041(1)	0.033(1)	-0.001(1)	0.0365(6)
Bi4	0	0.10499(5)	0.8982(2)	1	0.029(1)	0.028(1)	0.036(1)	0.003(1)	0.0310(6)
Bi5	0.5	0.26488(5)	0.8645(2)	1	0.033(1)	0.026(1)	0.031(1)	0.002(1)	0.0299(6)
Bi6	0.5	0.17709(5)	0.0368(3)	1	0.036(1)	0.033(1)	0.041(1)	0.001(1)	0.0366(6)
Bi7	0.5	0.51934(5)	0.8652(2)	1	0.031(1)	0.023(1)	0.033(1)	0.003(1)	0.0293(6)
Bi8	0	0.35944(6)	0.8998(2)	1	0.031(1)	0.035(1)	0.032(1)	0.002(1)	0.0324(6)
Bi9	0	0.44729(5)	0.7272(3)	1	0.040(1)	0.026(1)	0.048(2)	-0.002(1)	0.0378(7)
Bi10	0.5	0.23178(5)	0.3614(2)	1	0.030(1)	0.026(1)	0.030(1)	0.000(1)	0.0288(6)
Bi11	0	0.39190(5)	0.4033(2)	1	0.030(1)	0.024(1)	0.035(1)	0.000(1)	0.0294(6)
Pb1	0	0.06241(6)	0.2050(2)	1	0.038(1)	0.036(1)	0.026(1)	-0.003(1)	0.0335(6)
Pb2	0	0.18685(5)	0.7081(3)	1	0.041(1)	0.030(1)	0.045(2)	0.008(1)	0.0389(7)
Pb3	0.5	0.43728(5)	0.0540(3)	1	0.039(1)	0.028(1)	0.045(2)	0.004(1)	0.0373(7)
Pb4	0.5	0.31476(5)	0.5495(3)	1	0.038(1)	0.025(1)	0.049(2)	0.000(1)	0.0375(7)
Pb5	0	0.30960(5)	0.2145(3)	1	0.040(1)	0.022(1)	0.057(2)	-0.003(1)	0.0394(7)
Cu1	0	0.0100(2)	0.6080(6)	1	0.021(3)	0.050(4)	0.006(3)	-0.003(3)	0.025(2)
Cu2	0	0.2594(2)	0.6160(7)	1	0.038(4)	0.031(4)	0.040(4)	-0.002(3)	0.036(2)
Cu3	0.5	0.3652(2)	0.1472(10)	1	0.058(5)	0.022(4)	0.064(6)	0.011(4)	0.048(2)
Cu4	0.5	0.3858(2)	0.6530(9)	1	0.059(5)	0.023(4)	0.056(6)	-0.013(4)	0.046(2)
Cu5	0	0.2387(2)	0.1100(7)	1	0.038(4)	0.028(4)	0.040(4)	0.002(3)	0.035(2)
Cu6	0	0.4882(5)	0.112(2)	0.36(2)	0.04				
Cu7	0.5	0.1335(6)	0.656(2)	0.34(2)	0.04				
Cu8	0.5	0.1114(7)	0.150(3)	0.29(2)	0.04				
S1	0.5	0.1727(4)	0.500(1)	1	0.027(3)				
S2	0.5	0.0975(3)	0.334(1)	1	0.029(3)				
S3	0.5	0.0139(3)	0.163(1)	1	0.020(3)				
S4	0	-0.0469(3)	0.256(1)	1	0.022(3)				
S5	0	0.0305(4)	0.425(1)	1	0.028(3)				
S6	0	0.1108(3)	0.594(1)	1	0.023(3)				
S7	0.5	0.0747(4)	0.001(1)	1	0.030(3)				
S8	0.5	0.1512(3)	0.834(1)	1	0.026(3)				
S9	0.5	0.2348(3)	0.668(1)	1	0.024(3)				
S10	0	0.2962(3)	0.766(1)	1	0.020(3)				
S11	0	0.2181(3)	0.927(1)	1	0.022(3)				
S12	0	0.1367(3)	0.093(1)	1	0.019(3)				
S13	0	0.5491(3)	0.763(1)	1	0.028(3)				
S14	0	0.4719(4)	0.932(1)	1	0.033(4)				
S15	0	0.3881(4)	0.094(4)	1	0.034(4)				
S16	0.5	0.3264(4)	0.999(2)	1	0.038(4)				
S17	0.5	0.4059(4)	0.836(2)	1	0.040(4)				
S18	0.5	0.4869(4)	0.667(1)	1	0.031(4)				
S19	0	0.2003(3)	0.255(1)	1	0.023(3)				
S20	0	0.2772(3)	0.428(1)	1	0.027(3)				
S21	0	0.3613(4)	0.597(1)	1	0.027(3)				
S22	0.5	0.4228(4)	0.504(2)	1	0.038(4)				
S23	0.5	0.3464(4)	0.339(1)	1	0.031(4)				
S24	0.5	0.2617(3)	0.167(1)	1	0.025(3)				

Note that the data for Cu 7 and Cu 8 are taken from a subsidiary refinement in which Cu 6 was not included. The differences in parameters for the other atoms between the two refinements are negligible. sof: site-occupancy factor.

of the principal refinement. All the fully occupied atomic positions are essentially identical with those of the principal structure; the partly occupied Cu positions differ and will be described together with the corresponding positions from the principal structure.

DESCRIPTION OF THE STRUCTURE

The unit cell of $\text{Cu}_{10.7}\text{Pb}_{10.7}\text{Bi}_{21.3}\text{S}_{48}$ contains eight *en échelon* Me_4S_6 ribbons ($\text{Me} = \text{Bi}, \text{Pb}$) in two [010] rows

(Fig. 2). Six of them are “krupkaite-like ribbons”. However, in the principal structure, only four of these are pure krupkaite-like ribbons $\text{CuPbBi}_3\text{S}_6$, the remaining two have 0.36 Cu in the ideally empty copper site, corresponding to $(\text{Cu}_{1.36}\text{Pb}_{1.36}\text{Bi}_{2.64}\text{S}_6)$. The two “aikinite-like ribbons” $\text{Cu}_2\text{Pb}_2\text{Bi}_2\text{S}_6$ are situated at $y = 0.313$, $z = 0.382$ and $y = 0.687$, $z = 0.882$, respectively. If the partially occupied Cu sites are disregarded, *i.e.*, if the oversubstitution is removed, the structural formula of this four-fold derivative is $\text{Cu}_{10}\text{Pb}_{10}\text{Bi}_{22}\text{S}_{48}$ ($n_{\text{aik}} = 62.5$).

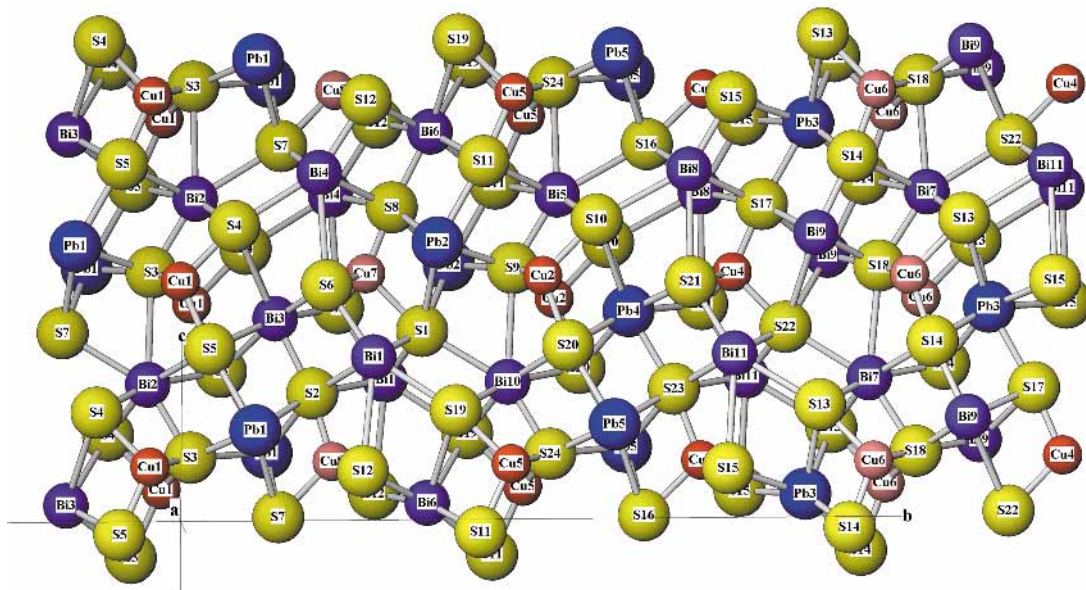


FIG. 1. A part of the emilite ($\text{Cu}_{10.7}\text{Pb}_{10.7}\text{Bi}_{21.3}\text{S}_{48}$) structure with the coordinations and atom labels. The lengths and directions of the half-axes are indicated.

The fully occupied Cu sites, Cu1–5, occur in zig-zag [001] rows, spaced either one half or a full subcell period ($b/4$) apart: the Cu1 row is at $y = 0.0$, the Cu2 and Cu5 rows at 0.25 (0.75), and the Cu3 and Cu4 rows at 0.375 (0.625) (Figs. 1, 2). In the principal crystal, the partly occupied Cu sites form a row at $y = 0.5$; the unoccupied rows are at $y = 0.125$ and 0.875.

The spacing of the adjacent [001] rows of fully occupied tetrahedra, a full subcell b parameter apart, is analogous to that in krupkaite, $\text{CuPbBi}_3\text{S}_6$; the spacing between rows that are $1/2$ subcell parameter apart corresponds to that in aikinite, CuPbBiS_3 . A fairly complicated sequence of these intervals results, krupkaite – krupkaite – aikinite – krupkaite – aikinite..., *i.e.*, single and double krupkaite-like intervals alternately occur in this sequence. Diffraction streaks parallel to b^* and the partly occupied Cu rows, different in the principal and the subsidiary crystals, bear witness to errors in this sequence.

Coordination polyhedra

The structure of $\text{Cu}_{10.7}\text{Pb}_{10.7}\text{Bi}_{21.3}\text{S}_{48}$ contains five fully occupied copper sites and one that is only partly occupied, and the corresponding adjacent five “pure” Pb positions and a mixed (Bi,Pb) site (called Bi9, and situated roughly at $y = 0.5$). All Pb-containing sites are the internal (central) cation sites of the ribbons. In addition,

there are two internal, pure bismuth sites, Bi3 and Bi6. There is a total of eight distinct terminal Bi sites distributed over the Me_4S_6 ribbons (Fig. 1).

Internal Bi sites in the ribbons have distinctly higher volumes of coordination polyhedra and of spheres circumscribed around the polyhedra than the marginal ones (Table 4). In this respect, they come close to Pb sites, from which they differ in having a higher eccentricity and a lower sphericity, although the volume-based distortion characteristics are about the same. The site Bi9, which we consider to be of mixed occupancy, differs only marginally from “pure” internal Bi sites by its slightly greater volume. Lead atoms have fairly uniform characteristics, except for the larger volumes of Pb4 and Pb5. This is caused by Pb1–3 being parts of krupkaite-like chains, similar to those in salzburgite (Topa *et al.* 2000), whereas Pb4 and Pb5 form part of aikinite-like chains (Table 5 in Topa *et al.* 2000). Among copper atoms, Cu3 is distinguished by the volume and eccentricity of its tetrahedron. It is followed by Cu2, with properties lying at the top of the scale defined by other Cu atoms (Table 4). Both Cu2 and Cu3 are located in the lateral tetrahedra of those krupkaite ribbons that are lodged between the aikinite-like ribbons.

In agreement with the findings of Berlepsch *et al.* (2001), the ratio V_P/V_S for Bi in the marginal positions is greater, *i.e.*, there is a higher efficiency of filling of the volume of the polyhedra than the central positions,

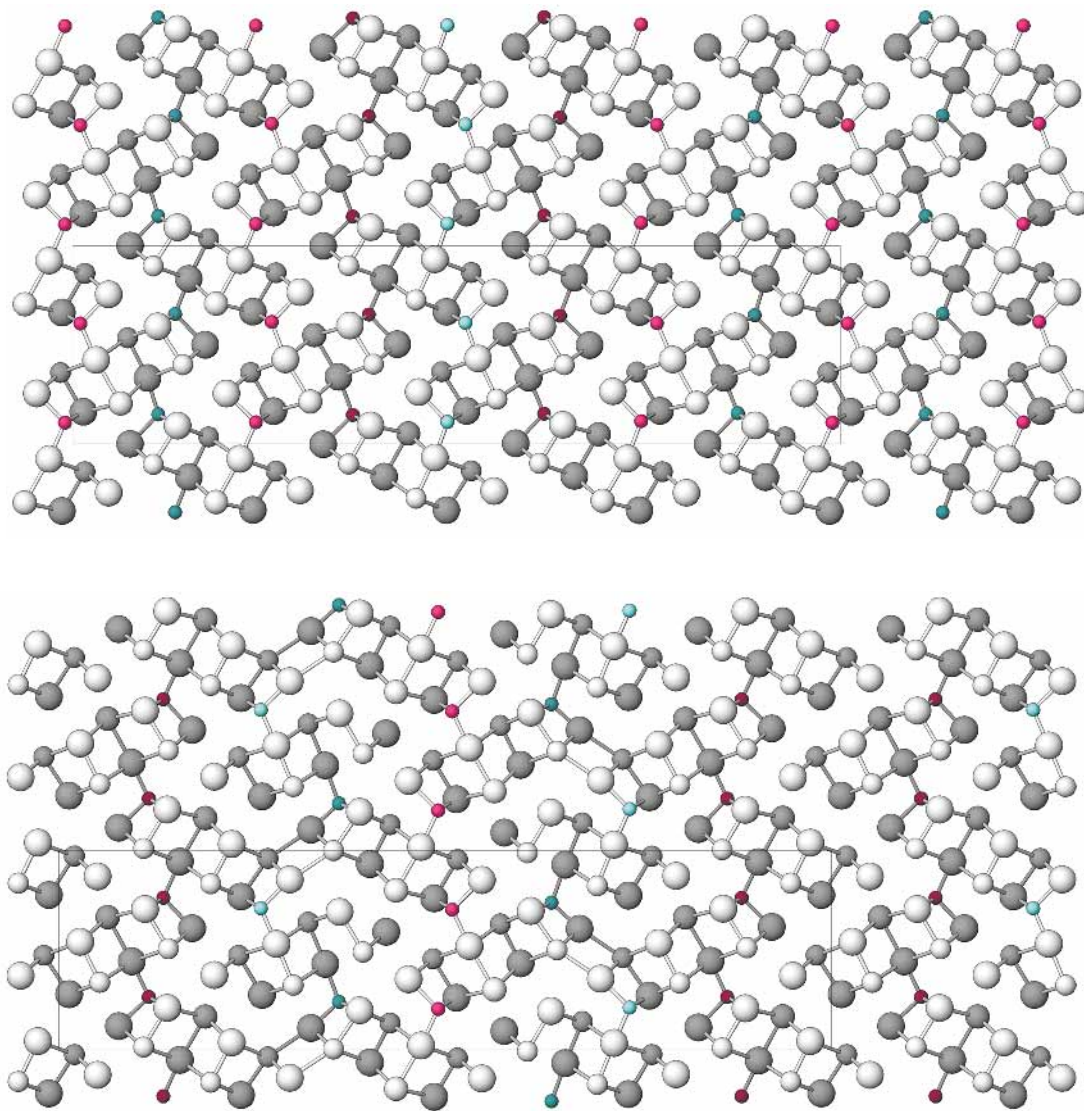


FIG. 2. A comparison of the structures of a) emilite ($\text{Cu}_{10.7}\text{Pb}_{10.7}\text{Bi}_{21.3}\text{S}_{48}$), and b) salzburgite ($\text{Cu}_{6.4}\text{Pb}_{6.4}\text{Bi}_{25.6}\text{S}_{48}$). Projections along $[100]$, b axis horizontal, c vertical. The atoms at two levels $\frac{1}{2}a$ period apart are shown as lightly and darkly shaded, respectively. In order of decreasing size, the atoms represent S, Pb, Bi, and Cu. The fully occupied Cu positions are indicated in red, and the positions refined as being partially occupied are blue. The origin of the unit cell for salzburgite has been translated $\frac{1}{2}b + \frac{1}{2}c$ with respect to the published data, for better comparison.

as shown by the values of volume-based distortion (Table 4), which are lower than for the internal sites.

Partly occupied Cu positions

On the basis of differences in the results obtained between the n_{aik} (67.5) and the n_{aik} (66.4) crystal, re-

spectively, refinements were repeated on the former, principal crystal, alternating the positions of subsidiary copper between the two non-equivalent sets of krupkaite-like intervals. The refinement with partly occupied Cu6 (0.0000, 0.4882, 0.112, occupancy 0.361) gave the agreement factor $R1 = 0.0661$ (Table 1), whereas that with alternative Cu positions [Cu7 (0.5000,

TABLE 4. POLYHEDRON DISTORTION PARAMETERS FOR CATIONS IN EMILITE

Atom	CN	Sphere radius	Sphere volume	Polyhedron volume	Volume distortion ⁽¹⁾	Eccentricity ⁽²⁾	Sphericity ⁽³⁾
Bi1	7	2.949	107.444	36.466	0.1031	0.4180	0.9009
Bi2	7	2.967	109.354	37.228	0.1003	0.3865	0.9343
Bi3	7	3.020	115.337	38.057	0.1280	0.4387	0.9396
Bi4	7	2.960	108.611	36.846	0.1035	0.3969	0.9206
Bi5	7	2.971	109.893	37.340	0.1021	0.4064	0.9426
Bi6	7	3.017	115.057	38.038	0.1263	0.4167	0.9536
Bi7	7	2.965	109.177	37.159	0.1006	0.3888	0.9259
Bi8	7	2.985	111.416	37.820	0.1030	0.4150	0.9624
(Bi,Pb)*9	7	3.029	116.458	38.492	0.1266	0.4478	0.9368
Bi10	7	2.969	109.667	37.245	0.1025	0.3996	0.9168
Bi11	7	2.963	108.944	37.021	0.1020	0.4229	0.9080
Pb1	7	3.031	116.697	38.479	0.1286	0.1324	0.9796
Pb2	7	3.039	117.529	38.775	0.1282	0.1778	0.9711
Pb3	7	3.036	117.198	38.748	0.1263	0.1922	0.9689
Pb4	7	3.066	120.698	39.972	0.1248	0.2736	0.9599
Pb5	7	3.074	121.644	40.326	0.1240	0.2332	0.9665
Cu1	4	2.357	54.838	6.509	0.0312	0.0596	1
Cu2	4	2.367	55.523	6.623	0.0263	0.0597	1
Cu3	4	2.376	56.181	6.686	0.0287	0.0993	1
Cu4	4	2.363	55.303	6.589	0.0275	0.0779	1
Cu5	4	2.355	54.691	6.498	0.0303	0.0701	1
Cu6	4	2.348	54.246	6.511	0.0203	0.1651	1
Cu7	4	2.358	54.937	6.598	0.0197	0.2212	1
Cu8	4	2.351	54.423	6.527	0.021	0.1538	1

The centroid parameters used are defined in Balić-Zunić & Makovicky (1996) and Makovicky & Balić-Zunić (1998). The volume distortions are calculated using the maximum volume polyhedra for respective CN (7 for a regular pentagonal bipyramid, 4 for a regular tetrahedron) as ideal reference.

(1) Volume distortion $v = [V(\text{ideal}) - V(\text{polyhedron})]/V(\text{ideal})$, to be multiplied by 100 to obtain percentage.

(2) "Volume-based" eccentricity $ECC_v = 1 - [(r_c - \Delta)/r_c]^3$, where r_c is the radius of the circumscribed sphere and Δ is the distance between the sphere center ("centroid") and the central atom.

(3) "Volume-based" sphericity $SPH_v = 1 - 3\sigma_v/r_c$, where σ_v is a standard deviation of the radius r_c .

* Compatible with a partly occupied Cu6 site.

0.1335, 0.656, occupancy 0.34) and Cu8 (0.5000, 0.1114, 0.150, occupancy 0.29] gave a very similar value, 0.0667.

The Cu–S distances in the Cu6 and Cu8 tetrahedra (Table 5) average at the lower end of the range observed for the principal tetrahedra Cu1–Cu5, whereas Cu7 lies within this range. However, all three tetrahedra Cu6–8 are distinguished by one very short Cu–S distance plus one or two distances close to the top of the observed range of Cu–S distances (Table 5), making the Cu6–8 tetrahedra distinctly more eccentric (Tables 4, 5) than those of the principal Cu atoms. The partly occupied Cu tetrahedra exhibit lower volume-based measure of distortion than the fully occupied ones (Table 4). Closest to the partly occupied positions in eccentricity are the Cu3 sites flanking krupkaite-like ribbons (Fig. 1, Table 4).

The coordination characteristics do not allow us to make a choice between the two alternative sets of subsidiary copper sites, although perusal of the listing of bond lengths suggests that Cu7 is most distorted and

TABLE 5. COPPER–SULFUR DISTANCES (Å) IN EMILITE

Atom	Distances			Average	Centroid-to-atom distance
	1×	2×	1×		
Cu1	2.311	2.372	2.386	2.360	0.048
Cu2	2.323	2.377	2.403	2.370	0.048
Cu3	2.380	2.347	2.447	2.380	0.081
Cu4	2.302	2.385	2.399	2.368	0.063
Cu5	2.320	2.356	2.409	2.360	0.056
Cu6	2.213	2.392	2.427	2.356	0.137
Cu7	2.216	2.372	2.530	2.373	0.189
Cu8	2.228	2.409	2.380	2.356	0.127

Cu8 has a rather unusual set of Cu–S distances. An attempt to refine all three sites simultaneously resulted in R1 equal to 0.0657, with occupancies of the three subsidiary sites equal to 0.31(2), 0.16(2), 0.13(2), respectively, and even poorer characteristics of the Cu7 and Cu8 coordination polyhedra.

We explain the variable and nearly equally probable configurations of partly occupied Cu sites as a result of structural faults in the structure of the phase examined, connected with its Cu–Pb oversubstitution compared to the ideal composition $\text{Cu}_{10}\text{Pb}_{10}\text{Bi}_{22}\text{S}_{48}$. These faults could occur as an occasional single krupkaite-like interval in place of the double one, bringing the adjacent undisturbed portions of the structure out of phase. Alternatively, they could occur as doubling of an aikinite-like interval, with similar consequences. Both types of faults would produce a twinning of the entire structure or of selected portions of it by inversion. Indeed, the Flack (1983) parameter, 0.50(3), suggests the presence of merohedral twinning. The structure was refined as a merohedral twin of approximately equal individuals related by the $\bar{1}$ operation. The 4–5% of n_{aik} oversubstitution compared to the idealized $\text{Cu}_{10}\text{Pb}_{10}\text{Bi}_{22}\text{S}_{48}$ composition requires a substantial proportion of structural faults of the above types, dislocating the basic structure into a number of (010) domains. Those rows of Cu sites in faulted (out-of-phase) regions, which are in excess of the inversion-related portions of the structure, cannot be accounted for by the refinement of the Flack parameter and will appear as partly occupied Cu portions in the bulk structure obtained by X-ray diffraction.

The multiple occurrence of faults that skip one out of two adjacent krupkaite-like intervals is probably preferred to a simple filling of rows of empty tetrahedra, which would create slabs of multiple aikinite-like intervals. The reason is that the phase examined is situated in the bismuthinite–aikinite series below hammarite, for which a simple sequence of intervals [krupkaite – aikinite – aikinite – krupkaite – aikinite] is typical. Multiple aikinite-like intervals are more likely for the phases with n_{aik} above that of hammarite.

An alternative explanation can be tentatively offered, analogous to the "Đurovič effect" defined recently by Nespolo & Ferraris (2001) for OD polytypes. The faults and portions with wrong intervals will contribute fully to the subcell reflections, to which also the ordered portions of the structure contribute, but their contribution to the supercell reflections will be marginal. In the perfectly ordered case, the contributions of supercell reflections to the Fourier summation modify the string of subcell structures in one supercell until the "wrong" Cu positions have been eliminated, reproducing the true ordered structure. If the two sets of reflections have different scale-factors owing to the different contributions to them by the non-ordered portions of the structure, the empty Cu positions will not be completely eliminated, and spurious Cu peaks will remain. If four non-centrosymmetric (krupkaite-like) subcells are juxtaposed filling the cell of the phase examined, starting with a plane of Cu sites positioned at 0.0, the imperfectly vacant Cu sites will produce virtual, partly occupied Cu positions at 0.5. If the same subcells are placed by starting over the central krupkaite-like interval, virtual Cu positions in the two paired krupkaite-like intervals will be produced instead. They do not have to represent real atoms, in good agreement with the indefinite behavior of spurious copper in the refinements quoted above. As Nespolo & Ferraris (2001) found, we cannot distinguish between the two cases, that of coherently diffracting out-of-phase blocks and the "Đurovič effect" produced by errors, without further work, *e.g.*, using the HRTEM approach. To the best of our knowledge, the "Đurovič effect" has not yet been recognized in the ordered derivatives of a structure, such as the bismuthinite–aikinite derivatives.

We believe that a certain amount of oversubstitution in the krupkaite modules might be required to secure their metric fit with the aikinite modules in one structure. However, because of the above-stated considerations, it is impossible to evaluate the percentage of Cu participating in the process of oversubstitution *versus* that present in structural defects.

Comparison with salzburgite, Cu_{6,4}Pb_{6,4}Bi_{25,6}S₄₈

The crystal structure of salzburgite (Topa *et al.* 2000) contains six krupkaite-like ribbons, CuPbBi₃S₆, and two bismuthinite-like ribbons, Bi₄S₆. The spacing of the latter is $\Delta y = 0.375$, just like that of aikinite-like ribbons in emilite. The inversion of the motif is underlined by the fact that the krupkaite-like ribbons in Cu_{10,7}Pb_{10,7}Bi_{21,3}S₄₈ are oriented toward one another in a way opposite to that in Cu_{6,4}Pb_{6,4}Bi_{25,6}S₄₈ (Fig. 2 in Topa *et al.* 2000). In this way, where one structure contains [001] rows of Cu-filled tetrahedra, the other has empty or half-empty tetrahedra (Fig. 2).

In salzburgite, Cu_{6,4}Pb_{6,4}Bi_{25,6}S₄₈, the intervals between two adjacent zig-zag rows of fully occupied tetrahedra are either $1\frac{1}{2} b_{\text{subcell}}$ dimension wide (an

interval which, by repetition, produces the structure of gladite) or one subcell *b* dimension wide (a krupkaite-like interval). They result in a simple sequence of two gladite-like intervals alternating regularly with one krupkaite-like interval. This simplicity contrasts with the complicated scheme described above of krupkaite- and aikinite-like intervals in emilite.

ACKNOWLEDGEMENTS

The research project on the crystal chemistry of sulfosalts and the diffraction equipment were financed by the Danish Natural Science Research Council. The support of the University of Copenhagen and the University of Salzburg is appreciated. Active interest and support of Prof. W. Paar (Salzburg), professional assistance of Mrs. Britta Munch and Mrs. Camilla Sarantaris as well as the helpful suggestions of the reviewers, Drs. A. Pring and N. Cook, and the editor, Prof. R.F. Martin, are gratefully acknowledged.

REFERENCES

- BALIĆ-ŽUNIĆ, T. & MAKOVICKY, E. (1996): Determination of the centroid or "the best centre" of a coordination polyhedron. *Acta Crystallogr.* **B52**, 78-81.
- BERLEPSCH, P., MAKOVICKY, E. & BALIĆ-ŽUNIĆ, T. (2001): Crystal chemistry of meneghinite homologues and related sulfosalts. *Neues Jahrb. Mineral., Monatsh.*, 115-135.
- FLACK, H.D. (1983): On enantiomorph-polarity estimation. *Acta Crystallogr.* **A39**, 876-881.
- MAKOVICKY, E. & BALIĆ-ŽUNIĆ, T. (1998): New measure of distortion for coordination polyhedra. *Acta Crystallogr.* **B54**, 766-773.
- _____, & MAKOVICKY, M. (1978): Representation of compositions in the bismuthinite–aikinite series. *Can. Mineral.* **16**, 405-409.
- _____, TOPA, D. & BALIĆ-ŽUNIĆ, T. (2001): The crystal structure of paarite, the newly discovered 56 Å derivative of the bismuthinite–aikinite solid-solution series. *Can. Mineral.* **39**, 1377-1382.
- NESPOLO, M. & FERRARIS, G. (2001): Effects of the stacking faults on the calculated electron density of mica polytypes – the Đurovič effect. *Eur. J. Mineral.* **13**, 1035-1045.
- PRING, A. (1995): Annealing of synthetic hammarite, Cu₂Pb₂Bi₄S₉, and the nature of cation-ordering processes in the bismuthinite–aikinite series. *Am. Mineral.* **80**, 1166-1173.
- TOPA, D., BALIĆ-ŽUNIĆ, T. & MAKOVICKY, E. (2000): The crystal structure of Cu_{1,6}Pb_{1,6}Bi_{6,4}S₁₂, a new 44.8 Å derivative of the bismuthinite–aikinite solid-solution series. *Can. Mineral.* **38**, 611-616.

Received July 1, 2001, revised manuscript accepted December 15, 2001.